JOURNAL OF MATERIALS SCIENCE 32 (1997) 4227–4235

Mechanosorptive effects in cellophane, polyamide 6 and some other polymers studied by dynamic mechanical analysis

P. R. EBRAHIMZADEH, J. KUBÁT
Department of Polymeric Materials, Chalmers University of Technology, S-412 96 Gothenburg, Sweden

Dynamic mechanical data obtained in the tensile mode with cellophane, polyamide 6, PEO, PVAc and PUR foam (compression) subjected to stepwise humidity changes between 5% and 85% relative humidity are reported. With the exception of PVAc, the loss tangent, tan δ, shows a transient peak every time the relative humidity of the surrounding atmosphere is changed. The strength of the tan δ transients increases when the measuring frequency is lowered. The tan δ transients slowly disappear in response to reduction of the rate of humidity change. High amplitude and prestress with static load reduce the height of the transient peaks. Long-term testing results in relatively small changes in the shape of the loss tangent versus time data. For PA6 a narrowing of the loss tangent peaks with diminishing specimen thickness was observed.

1. Introduction

Mechanosorption is a collective term denoting certain characteristic changes in the mechanical behaviour of hygroscopic solids subjected to cyclically changing humidity of the surrounding atmosphere. The most well-known characteristic of such phenomena is the accelerated creep of wood exposed to a changing humidity. In the simplest case when the humidity is changed between two levels only, the overall creep rate is significantly higher than that corresponding to the higher humidity level. Effects of this type have an obvious impact on the use of wood in structural applications. Another example of the practical significance of this type of synergy between time-dependent mechanical behaviour and sorption is the compression–creep collapse of stapled corrugated boxes. Problems of this type are always to be expected because constant humidity is a condition prevailing only in laboratories.

Not surprisingly, the bulk of the publications in this area relate to accelerated creep of wood under sorption and desorption of water vapour [1–5]. Interest in these effects in the area of paper and paper-based packaging materials is of a more recent date [6–9].

As already mentioned, mechanosorption is not limited to cellulose and cellulose-based composites. It is an effect common to hygroscopic materials and substances in general. The reader will find an overall picture of such phenomena elsewhere [10–12]. Although creep, both in the tensile and bending modes, is the preferred method when approaching these phenomena experimentally, there are reports on using methods such as dynamic-mechanical instrumentation (DMA) applied, for instance, to paper [13, 14]. A basically similar method has also been employed in a study of the behaviour of Scots pine veneer and some other wood species [15]. The main finding was the appearance of pronounced peaks in the damping capacity, expressed as tan δ, that is the ratio between the loss and storage moduli. Such peaks, although of different shape, were observed both upon humidification and drying. In addition, an acceleration of the rate of stress relaxation was found. The relative humidity, RH, was periodically changed between 5% and 85%.

In a subsequent paper [16], dealing with Scots pine veneer and paper, the maxima in tan δ were subjected to a closer study, supplemented by thermogravimetric measurements (TGA). An approximately linear relation was found between the rate of sorption/desorption and the shape of the tan δ peaks. Another observation was an increase in the intensity of the damping peaks with decreasing frequency of the dynamic-mechanical testing device. Decreasing the rate at which the humidity was changed produced a reduction in the height of the peaks. Simultaneously with tan δ, also the variation of the force to deform the sample was recorded and evaluated. The bulk of the experiments related to the three-point bending mode. With paper and thin wood specimens, the tensile mode was employed, yielding largely equivalent results.

The present paper is a similar study, extending the range of hygroscopic polymers studied by DMA to cellophane and polyamide 6 (PA6) as well as poly(ethylene oxide) (PEO), water blown polyurethane foam (PUR) and poly(vinyl acetate) (PVAc).

0022–2461

The focus of this paper is on the behaviour in the tensile mode of the tan δ peaks and the corresponding variation of the force needed to deform the sample (the PUR specimens were tested in compression). The results are basically equivalent to those observed earlier with wood. They show that mechanosorptive effects are not related to the particular fibre architecture of wood or paper as is sometimes believed, but are a general feature of materials exhibiting a sufficient level of hygroscopicity, including materials with semicrystalline structures like cellophane and PA6.

2. Experimental procedure

The samples used in this investigation were as follows. The cellophane films, of thickness 20 and 40 μm, contained plasticizing additives. The amount of water-extracted plasticizer was 11% and 15%, respectively (Soxhlet extraction). The plasticizer was a mixture of glycerol (40%) and a poly(ethylene oxide) adduct, the nature of which could not be determined. Several other substances present in small amounts and appearing in mass spectrographic recordings also remained unidentified. The degree of polymerization of the regenerated cellulose constituting the film was 570, as determined by viscometry of a copper ethylenediamine solution (SCAN-C 15 : 62).

The polyamide 6 specimens (SNIA Technopolimeri spa.) were 20, 30 and 52 μm thick non-oriented cast films with a density of 1.13 $g\,cm^{-3}$. Their water absorption was 3.4% at 23 °C/50%RH. The average number molecular weight was 27 000.

Poly(ethylene oxide) from Scientific Polymer Products, Inc. had an M_W of 200 000. It was used in the form of 0.13 mm thick isotropic plaques compression moulded at 80 °C.

PVAc (Mowilith, Hoechst AG) with molecular weight M_W 260 000 and a density of 1.195 $g\,cm^{-3}$ was compression moulded at 130 °C to isotropic sheets with a thickness of 0.15 mm.

The water-blown PUR foam was based on a mixture (approximately 2 : 1) of polyoxialkylenetriol (viscosity 1.55 Pa s at 20 °C) and modified diphenylmethane-4.4'-diisocyanate (MDI) containing smaller amounts of accelerators and catalysts. The density of the foam was 0.087 $g\,cm^{-3}$.

The degree of anisotropy of the cellophane and PA6 films was determined as the ratio of tensile moduli measured in the longitudinal and transverse directions (RSAII device, cf. below, strain rate 0.1% s^{-1}, 20 °C, 40% RH). The results were as follows: cellophane 20 μm $E_{//}/E_{\perp}$, 13.3/10, cellophane 40 μm 7.7/3.8 (modulus values given in GPa). The corresponding ratios for the 20, 30 and 52 μm PA6 films were 2.5/2.4, 3.0/2.7 and 2.7/2.7, respectively. The PA6 specimens thus showed a significantly higher degree of isotropy than the cellophane material.

For cellophane, the direction in which the samples in the various experiments were cut is specified in connection with the corresponding results. For PA6, such a specification was not considered necessary.

The different degrees of anisotropy of the cellophane and PA6 specimens are also reflected in the dimensional changes determined when changing the relative humidity in both directions between the two humidity levels used in the DMA measurements, that is 5% and 85% RH.

For cellophane, 20 μm thick, the average change in thickness due to swelling was around 5.4%. The dimensional changes in the longitudinal and transverse directions were 2.2% and 2.4%, respectively. The corresponding figures for the 40 μm film were 7.1%, 2.8% and 6.2%. For the PA6 films, the thickness changed by around 1.2%, while the longitudinal and transverse swelling resulted in a dimensional change of around 3%. Obviously, the changes in sample dimensions on humidification or drying affect the force required to produce a given strain. However, for the as-received cellophane and the PA6 the changes in the force on humidification or drying are much larger than can be ascribed to such dimensional change alone. Instead, the dominant cause of the change in the registered force on humidification or drying is the change in the Young's modulus of the sample. By inference, this is true of the PEO film as well, but not necessarily true of the PVAc film.

DSC measurements (Mettler M3) carried out with PA6 specimens of different thicknesses did not reveal any significant differences in the melting temperature range.

The dynamic mechanical measurements (DMA) were carried out using a Rheometrics Solids Analyser RSA II operated in the tensile mode for all the samples except PUR, where compression loading was used. This instrument and experimental procedure have been described in detail elsewhere [15]. The effective length and width of the samples tested in the tensile mode were 22 and 2.5 mm, respectively.

The PUR specimens were cylindrical in shape with a diameter of 15 mm and a thickness of 3.6 mm.

All results presented below relate to humidity cycling between 85% (humid air) and 5% (nitrogen) as described elsewhere [15]. The normally used flow rate through the measuring chamber (volume 270 ml) enclosing the specimen was 1 l min^{-1}. The normally used frequency was 1 Hz.

3. Results

3.1. Cellophane

Fig. 1 shows the tan δ peaks obtained upon drying and humidification of the 40 μm thick cellophane sample, that is after exposure of the specimen to the two RH levels used. It is seen that distinct, narrow tan δ peaks are recorded both upon drying and humidifying. In this respect cellophane behaves differently from the Scots pine veneer specimens studied earlier [15, 16], where such behaviour was noted only when RH was suddenly raised to 85%. From Fig. 1, it further follows that the overall damping level tends to increase with the humidity, as normally expected for hygroscopic polymers.

The corresponding force diagram in the lower part of Fig. 1 shows higher force (stress) levels at lower RH as expected. The amplitude of the applied periodic strain deformation is given in terms of a percentage of

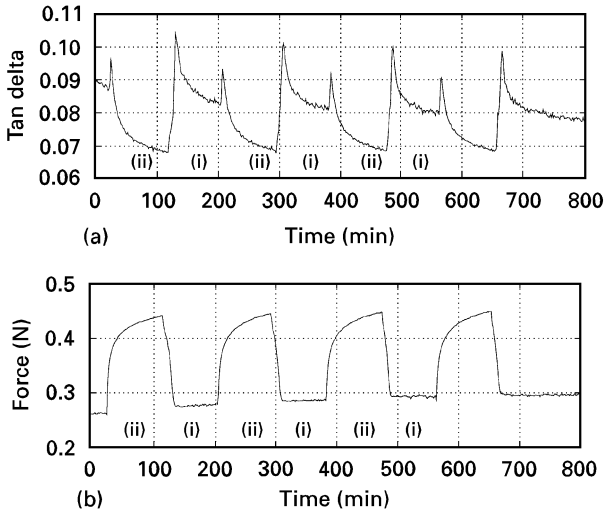

Figure 1 Variation of (a) the loss tangent (tan δ) and (b) tensile force in dynamic mechanical measurements during periodic humidity changes between (i) 85% and (ii) 5% RH for 40 μm thick cellophane, cut in the transverse direction. Frequency 1 Hz, strain amplitude 0.09%, pre-tension 30 g.

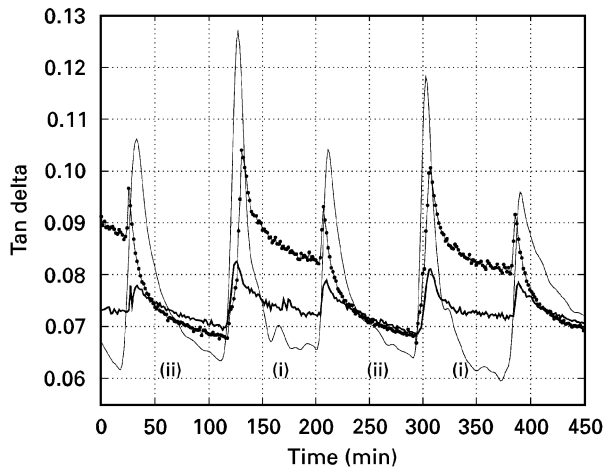

Figure 2 Effect of frequency on tan δ peaks for 40 μm cellophane (transverse direction) during humidity cycling (period about 90 min) between (i) 85% and (ii) 5% RH. These RH levels apply to all subsequent figures. Strain amplitude 0.09%, pre-tension 30 g. Frequency: (——) 0.1 Hz, (●) 1 Hz, (——) 10 Hz.

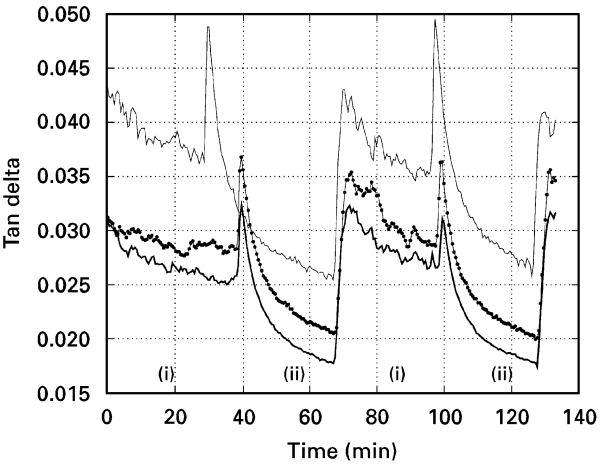

Figure 3 Effect of amplitude on tan δ for 20 μm cellophane (longitudinal direction) during humidity cycling (period about 30 min). Frequency 1 Hz, pre-tension 15 g. Strain amplitude: (——) 0.08%, (●) 0.25%, (——) 0.48%.

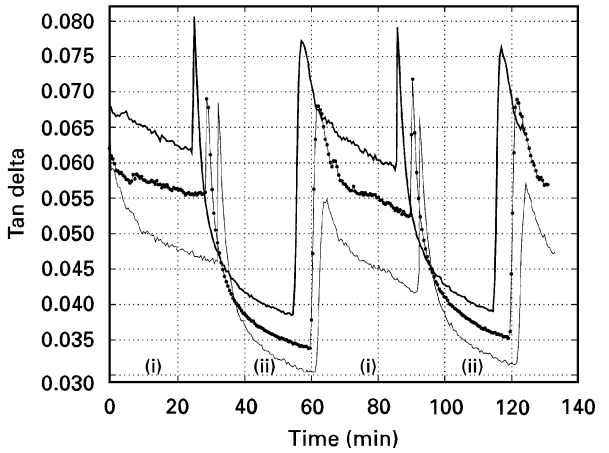

Figure 4 Effect of pretension on tan δ for 20 μm cellophane (longitudinal direction) during humidity cycling (period about 30 min). Frequency 1 Hz, strain amplitude 0.12%. Pre-tension (——) 30 g, (●) 60 g, (——) 150 g.

the sample length, that is, $100\delta l/l$. There is also an indication of an overall increase of the force as the humidity cycling proceeds.

Similarly to the pine veneer samples studied earlier [15, 16], the intensity of the damping peaks recorded with cellophane exhibited a distinct dependence on the measuring frequency, higher peaks being observed as the frequency was lowered. This is illustrated in Fig. 2 for 10, 1 and 0.1 Hz for the same specimens as used in Fig. 1.

As reported earlier [16] the intensity of the transient damping peaks diminished with increasing oscillation amplitude of the DMA device. In Fig. 3 we illustrate a similar effect observed with cellophane. Although the strain amplitude range was relatively limited, varying from 0.08%–0.48%, its influence is substantial. In these experiments, the thinner cellophane grade (20 μm) cut in the longitudinal direction was used. It is seen that upon drying a more distinct, sharper peak is recorded than in the case when RH is suddenly raised to 85%, where the peak is lower and broader. In this respect 20 μm specimens behave differently from the 40 μm transversally cut cellophane and Scots pine veneer samples used earlier [15, 16], where the tan δ response to RH changes showed the opposite behaviour. The applied pre-stress was around 3 MPa.

The same cellophane grade was used in experiments at varying pre-stress. The results, reproduced in Fig. 4, show a distinct increase in the intensity of the damping transients with the pre-stress level.

When used as-received cellophane (40 μm, transversally cut) contains plasticizing additives. Owing to their hygroscopicity, the latter compounds serve to reduce the brittleness of the cellulosic material. Extraction of the plasticizing component, as described in Section 2, may thus be expected to affect the damping behaviour. Fig. 5 shows that this is, in fact, the case, the tan δ values of the extracted specimens (40 μm, transversally cut) lying significantly below those of the

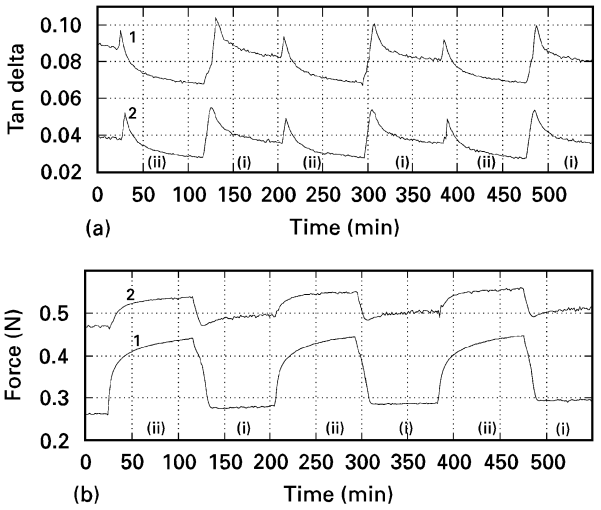

Figure 5 (a) Tan δ and (b) tensile force of 40 μm cellophane (transverse direction) with and without plasticizing components extracted during humidity cycling (90 min). Frequency 1 Hz, amplitude 0.09%, pre-tension 30 g. (1) As-received, (2) extracted.

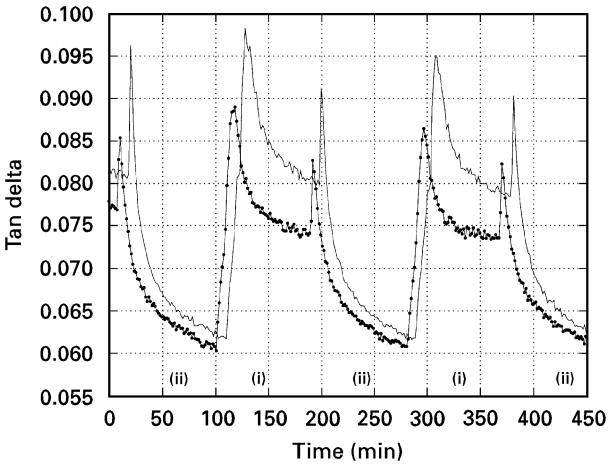

Figure 6 Tan δ for 40 μm cellophane (transverse direction) (——) before and (●) after 3 d continuous testing. Humidity cycling (period 90 min). Frequency 1 Hz, amplitude 0.09%, pre-tension 30 g.

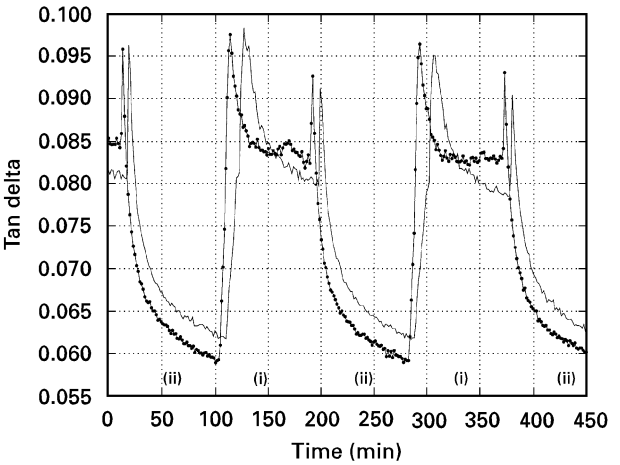

Figure 7 Tan δ for 40 μm cellophane (transverse direction) (——) before and (●) after 24 h DMA testing at a pre-tension of 30 g followed by 48 h unloading. RH cycling (period 90 min) during the whole 72 h period. Frequency 1 Hz, amplitude 0.09%.

as-received specimen. The corresponding force–time data measured at varying RH levels for the two cellophane specimens are shown in the lower part of Fig. 5. Obviously, the plasticizer has a strong influence on the dynamic mechanical properties of cellophane.

Comparison of the tan δ data for 40 μm cellophane (strain amplitude 0.09%, frequency 1 Hz) in Fig. 2 with corresponding data for 20 μm cellophane (strain amplitude 0.08% frequency 1 Hz) in Fig. 3 shows that the width of the tan δ peak is smaller for the thinner sample.

When studying the damping behaviour of the Scots pine samples [16], a marked dependence of the tan δ transients on the time period elapsed since the beginning of the measurement was found. We therefore carried out experiments intended to reveal possible effects of this type for cellophane. The specimen was subjected to both mechanical vibrations (1 Hz, strain amplitude 0.09%) and periodic humidity changes (period 90 min) for 3 d, whereafter the recording reproduced in Fig. 6 was made. When comparing this result with that of the experiment carried out in the usual way, we find a distinct lowering of the peak intensity and the overall damping level for the humidification period. The same applies to the height of the damping peaks measured during the drying period. However, there is no marked difference in the following development of the damping level. The sample used here was transversally cut and 40 μm thick.

In a similar long-term experiment, the same cellophane grade was subjected to mechanical vibrations (1 Hz, strain amplitude 0.09%) and humidity changes (period 90 min) for 24 h. Thereafter the vibrations were switched off and the sample kept for 48 h without pre-stress, exposed only to the periodically varying RH. As follows from Fig. 7, the result obtained following this pretreatment was different from that discussed above. In the latter case the tan δ peak height remained unaffected during the high RH period, while during drying the loss tangent level fell at a slightly higher rate.

3.2. PA6

The next set of data relates to experiments carried out with PA6 film. Owing to the high flexibility of the samples, the tension mode was used also in this case. Fig. 8 shows the results of the basic DMA experiment with the 52 μm thick PA6 grade, that is the response of tan δ and the force amplitude to sudden changes in RH between 5% and 85%. Also in this case, there are distinct damping peaks every time the humidity is varied. In contrast to cellophane, the peaks observed upon humidification are narrower than those resulting from a drying step. From the variation of tan δ with time, one may conclude that the desorption process takes place at a lower rate than that of water uptake. The level which tan δ tends to assume with time is in agreement with the expected behaviour, implying that the damping capacity increases with humidity. This is also true of the variation of the force amplitude, where a distinct increase is observed as the humidity is lowered, cf. Fig. 8b, lower part.

In Fig. 9 we illustrate the role of the rate of humidity exchange around the 52 μm thick PA6 sample. The

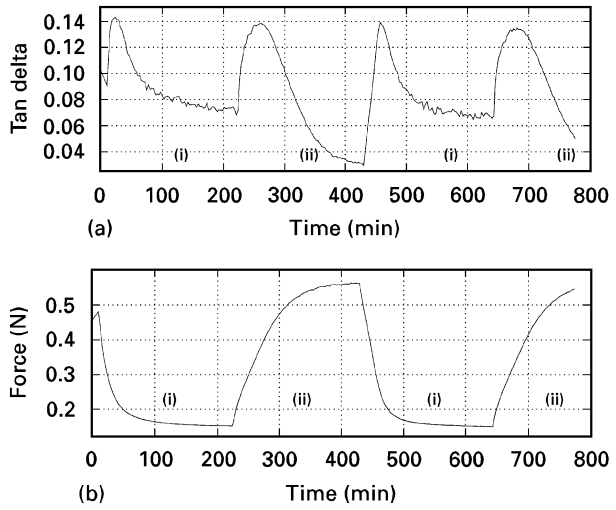

Figure 8 (a) Tan δ and (b) tensile force for 52 μm PA6 film during humidity cycling (period about 210 min). Frequency 1 Hz, strain amplitude 0.09%, pre-tension 30 g, flow rate 2 l min^{-1}.

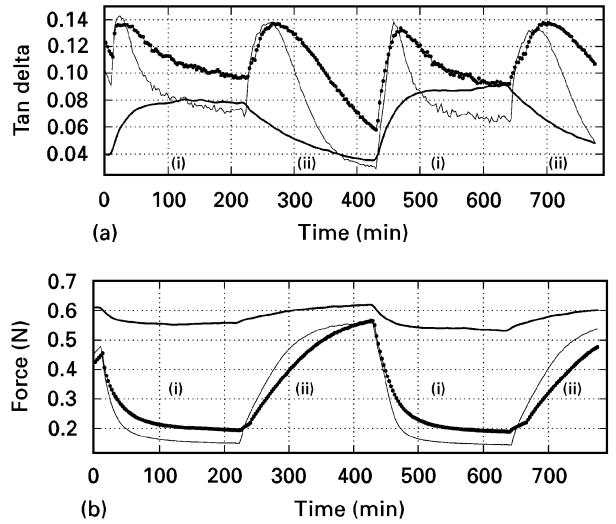

Figure 9 Effect of the rate of humidity change on (a) tan δ peaks and (b) tensile force for 52 μm PA6 film during humidity cycling. Frequency 1 Hz, amplitude 0.09%. Flow rates: (——) 2.0 l min^{-1}, (●) 0.2 l min^{-1} and (▬) 0.02 l min^{-1}.

flow rate at which the dry/humid nitrogen is blown into the sample chamber has a considerable effect on the variation of the loss tangent with time. Although the data of Fig. 9 only relate to three flow rates, they provide a relatively clear picture of the effect of the flow rate on the damping response. The narrowest damping peaks are observed at the highest flow rate used, that is 2 l min^{-1}. Because the sample chamber had a volume of 270 ml, the time needed to replace the atmosphere around the sample was about 8 s. Reducing the flow rate by a factor of 10 resulted in a substantial broadening of the damping transients, the differences in shape between the peaks observed on humidification/drying remaining largely similar. However, an entirely different pattern is found for the lowest rate used, amounting to 1% of the highest one. In this case, no peaks in the damping capacity were recorded. The damping varied as expected with the humidity, the above mentioned asymmetry between

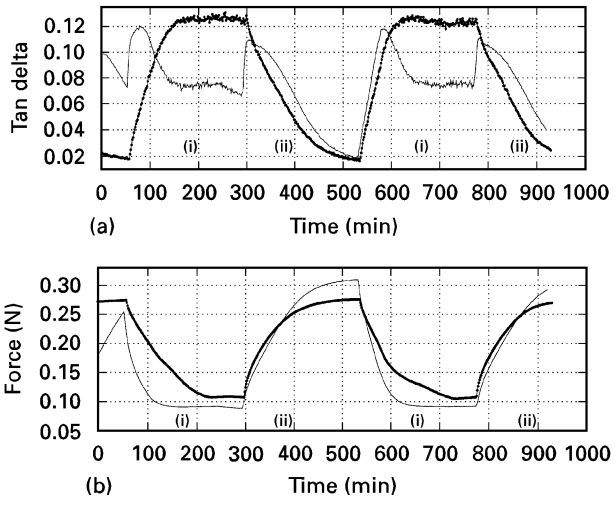

Figure 10 Effect of pre-tension on (a) tan δ and (b) tensile force for 52 μm PA6 film during humidity cycling (period about 210 min). Frequency 0.1 Hz, strain amplitude 0.09%, pre-tension (——) 30 g, (●) 180 g.

the sorption and desorption processes being clearly discernible. It may be noted that a flow rate of 1 l min^{-1} was used in most of the experiments presented in this paper. This applies also to the data shown elsewhere [15, 16] for pine wood and paper.

In the experiments with Scots pine veneer in the three-point bending mode, we found that the transient damping peaks tend to diminish in height when the amplitude of the vibration is increased or when the specimens are pre-stressed in the direction of the vibrations. In Fig. 10 we illustrate a similar effect found in the tensile mode with pre-stressed PA6 samples (52 μm thick). While the data of Figs 8 and 9 relate to a pre-stress of 30 g (2.3 MPa), necessary to allow the DMA device to work properly, the results shown in Fig. 10 were obtained at pre-stress levels of 30 g (2.3 MPa) and 180 g (13.9 MPa). When comparing these results with corresponding data for cellophane, Fig. 4, we find that the two polymers behave differently. With cellophane, a distinct increase in the peak intensity was found at higher pre-stress levels.

When considering the results of Fig. 10 for PA6, one notes that although there are no damping peaks at the highest pre-stress, the damping still reaches the peak values of the transients observed when the pre-stress is lower. The differences in the corresponding force–time diagrams between the differently prestressed specimens were rather small. They are therefore not reproduced here.

The enhancement of the damping transients by lowering the vibration frequency is illustrated in Fig. 11 for the PA6 specimen pre-stressed in the tensile mode with 60 g (4.6 MPa), cf. Fig. 10. As can be seen, distinct tan δ peaks, eliminated at a frequency of 1 Hz by this pre-stress level, reappear when the frequency is reduced to 0.01 Hz. As expected, the force amplitude at this frequency was somewhat lower (not shown here).

A similar effect was recorded when the pre-stress was increased to 180 g (13.9 MPa). Also in the latter

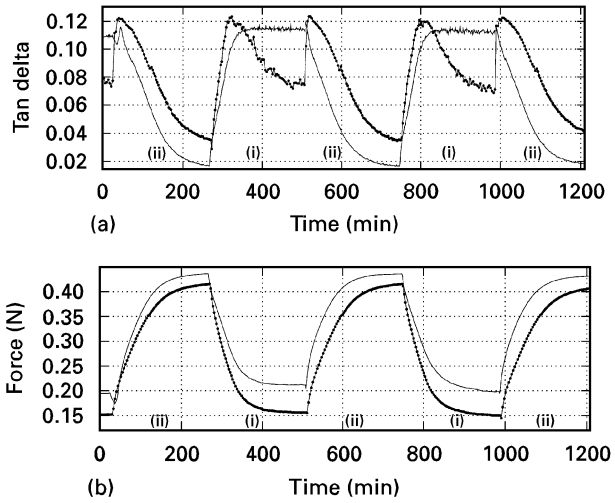

Figure 11 Effect of frequency on (a) tan δ peaks and (b) tensile force for 52 μm PA6 film during humidity cycling (period about 90 min). Strain amplitude 0.12%, pre-tension 60 g. Frequency: (——) 1 Hz, (●) 0.01 Hz, amplitude 0.09%.

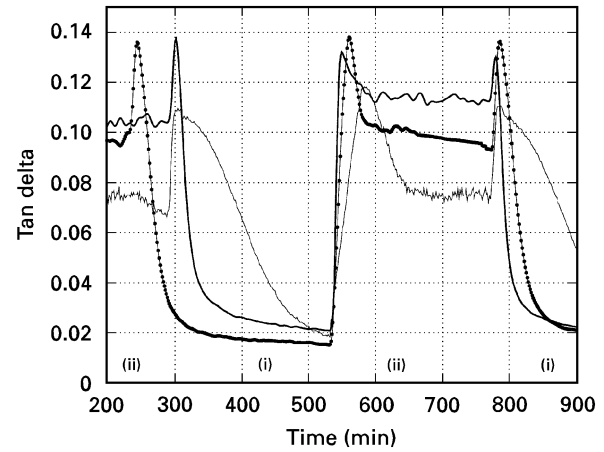

Figure 12 Effect of the PA6 film thickness on tan δ peaks during humidity cycling. Strain amplitude 0.09%, pre-tension 30 g. Frequency 0.1 Hz. Thickness: (——) 52 μm, (●) 30 μm, (——) 20 μm.

case, the height of the tan δ peaks at 0.01 Hz was approximately equal to the damping levels reached with the pre-stressed samples at 1 Hz, where no peaks were recorded.

Considering the close relationships between the damping transients and the sorption/desorption rate, as demonstrated for the Scots pine specimens in [16], it may be expected that the form of the transients will be affected by sample thickness. The data shown in Fig. 12 for PA6 with three different thicknesses (20, 30 and 52 μm) and a frequency of 0.1 Hz demonstrate that this, in fact, is the case. The two thinnest samples yield the narrowest peaks, while the peak measured with the 52 μm film is substantially broader following both sorption and desorption. The differences in the damping levels of the humidified sample remain unaccounted for at present because the structural characteristics of the samples have not been studied.

The corresponding force–time diagrams do not reveal any significant differences between the samples with varying thickness. Because the amplitude of the 0.1 Hz vibration was the same in all experiments, the force is found to be rather closely proportional to the thickness.

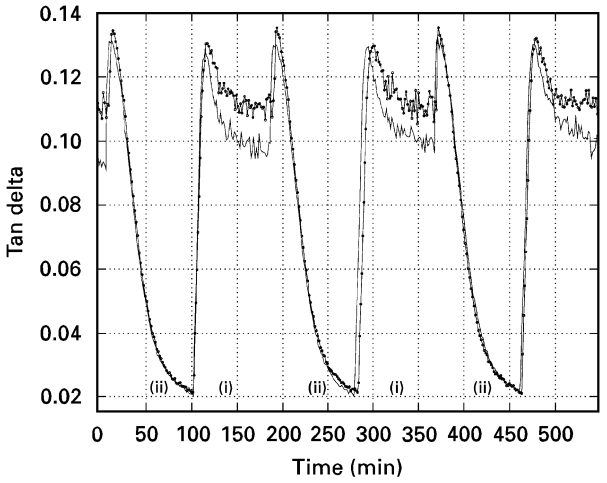

Figure 13 Tan δ for 30 μm film PA6 (——) before and (●) after 3 d continuous testing and humidity cycling (period 90 min). Frequency 0.1 Hz, pre-tension 30 g.

When repeating the experiments shown in Fig. 12 with a vibration frequency of 1 Hz, only the 52 μm specimen exhibited the damping transients, while no such effects were found with the two thinner films.

A set of long-term data, similar to that shown above for cellophane, was obtained also for the 30 μm PA6 film. The results, Fig. 13, show that, in contrast to cellophane, the damping level increases somewhat during the 85% RH period after a measuring time of 3 d. However, similarly to the behaviour of cellophane, the development of tan δ with time during drying is not measurably affected by subjecting the specimen to 3 d continuous vibration and periodic humidity changes. It may be remarked that the frequency used in this case was 0.1 Hz, while that employed in the experiments with cellophane was 1 Hz. The choice of a lower measuring frequency for PA6 was dictated by the absence of damping transients at 1 Hz for the 30 μm PA6 grade.

3.3. PEO

Another hydrophilic polymer included in this study is poly(ethylene oxide) (PEO), the dynamic-mechanical behaviour in the tensile mode of which is shown in Fig. 14. We note that the transient damping peaks are narrower and higher during the drying interval. In this respect PEO behaves similarly to cellophane. The opposite was recorded with PA6, Fig. 8, and with wood and paper [16].

3.4. PUR

The next substance selected for the basic type of experiments presented here was water-blown polyurethane foam, PUR, a material with a relatively low water absorption of about 5% at 85% RH. Although

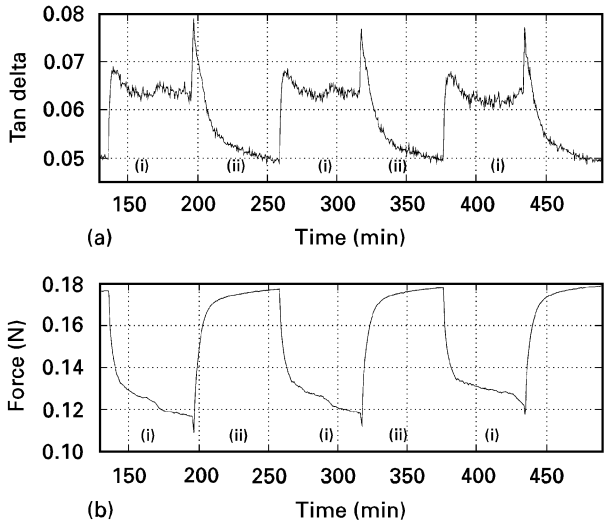

Figure 14 (a) Tan δ and (b) tensile force for PEO during humidity cycling (period about 90 min). Sample thickness 0.13 mm, frequency 1 Hz, amplitude 0.09%.

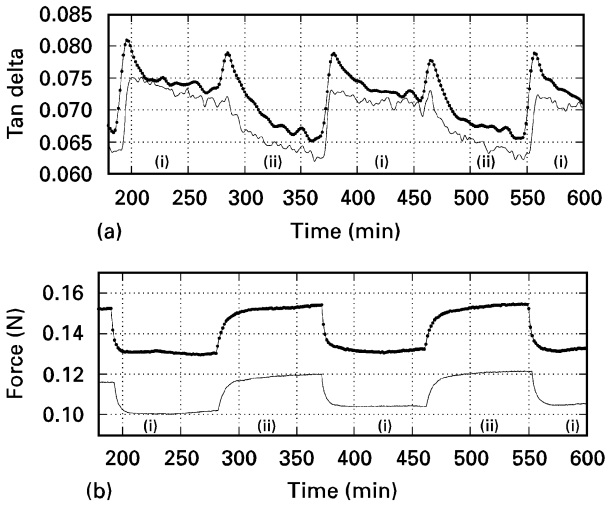

Figure 15 (a) Tan δ and (b) tensile force for water-blown PUR foam during humidity cycling (period 90 min). Uniaxial compression, cylindrical sample, diameter 15 mm, thickness 3.6 mm. Strain amplitude 0.12%, pre-tension 500 g. Frequency: (——) 1 Hz, (●) 0.01 Hz.

the DMA results of Fig. 15 show a distinct variation of the force amplitude with the RH level, no peaks appear in the corresponding damping diagrams at the usual frequency of 1 Hz. However, when reducing the frequency of the vibrations to 0.1 Hz, the tan δ peaks are recovered, albeit to a relatively small extent. The experiments in question were carried out in the compression mode. Accelerated creep of PUR foam during cyclic humidity changes has been reported earlier [17].

3.5. PVAc

Poly(vinyl acetate) (PVAc) is a polymer with a lower water absorption than the materials treated above. Its behaviour in the usual DMA experiments is illustrated by the data shown in Fig. 16. Although the variation in the RH level produces distinct changes in both tan δ and the force amplitude, no damping transients are visible on the tan δ diagram recorded at 1 Hz. When reducing the measuring frequency to 0.01 Hz, known

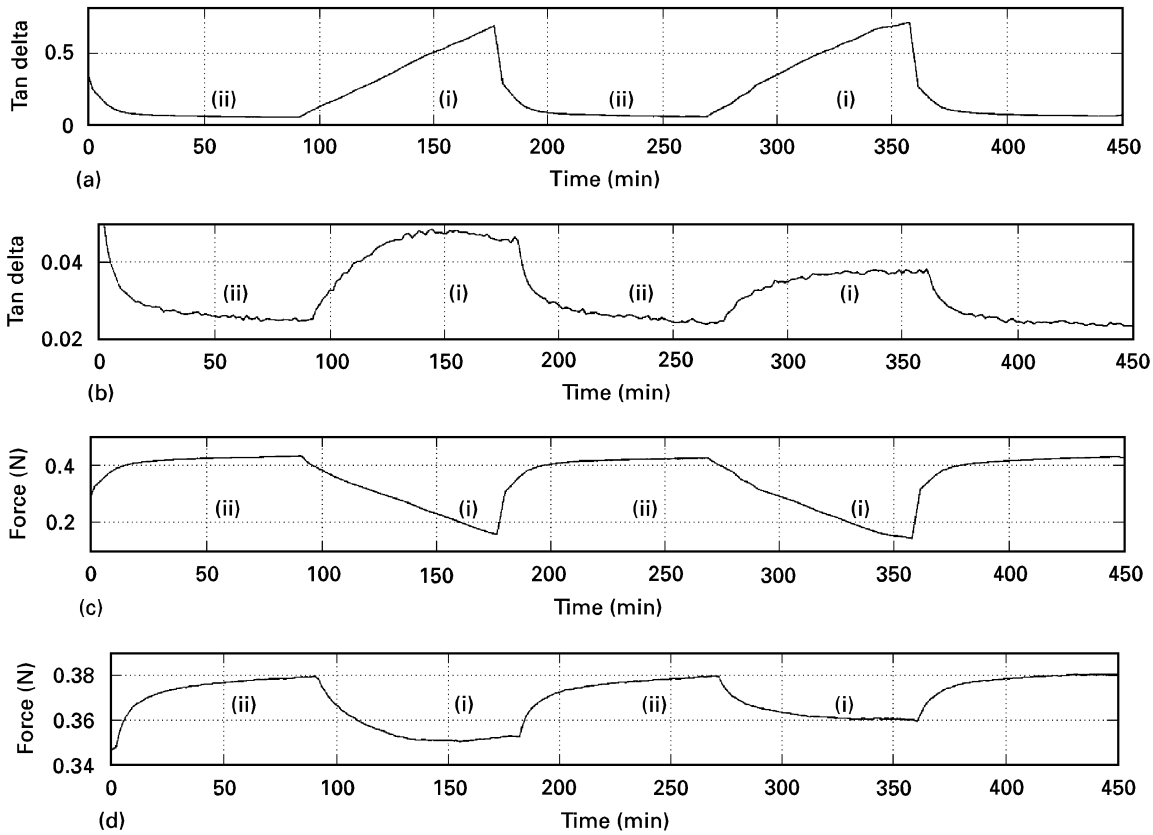

Figure 16 (a, b) Tan δ and (c, d) tensile force for PVAc during humidity cycling (period about 90 min). Uniaxial tension, sample thickness 0.15 mm, strain amplitude 0.09%, pre-tension 30 g. Frequency: (a, c) 0.01 Hz and (b, d) 1 Hz.

from the data presented above to enhance the appearance of the damping transients, no change in the damping behaviour is noted. However, there is a significant deformation of both the $\tan\delta$–time and force–time diagrams, as is evident from Fig. 16. In addition, the time range of the variation of both these variables is significantly increased. This is likely to be due to the viscoelasticity of this material, which is especially pronounced because the measuring temperature is rather close to the glass transition temperature at around 30 °C.

4. Discussion

Mechanosorptive phenomena represent a highly complex interplay between viscoelastic effects and sorption/desorption processes. An additional factor making the quantitative evaluation of results obtained even more difficult, is the dimensional changes following from the varying humidity content of the specimens. The application of conventional dynamic mechanical testing, as reported in the present paper, thus necessarily yields results where the role of dimensional changes cannot be taken into proper account. In the first place, this applies to the two key parameters of such measurements, that is the storage and loss moduli. This is the reason why, in some of the above diagrams, we supplement the variation of the loss factor, $\tan\delta$, at varying RH with the corresponding force diagram. For the same reason, $\tan\delta$ is clearly to be given preference before the loss modulus. Because the former quantity is the ratio of the loss and storage moduli, it may be expected to remain unaffected by changes in the dimensions of the specimen.

The results presented above are intended to provide a qualitative demonstration of the general character of the damping transients accompanying changes in the humidity content of the material being studied. Although the concurrent dimensional changes due to the swelling/shrinkage of the samples have not been determined, they would not affect the damping pattern observed in any appreciable way. The results are in agreement with similar data obtained in dynamic mechanical experiments with Scots pine veneer and some other wood species [15, 16]. At the same time, they extend the range of hygroscopic materials exhibiting this type of effect.

As is evident from the results, the degree of hygroscopicity of the specimens used is a key parameter in the present context. This is to be expected on grounds of specific interactions between the humid atmosphere and the hydrogen bonds of the material. Other molecules capable of interacting with such bonds, such as, ammonia, have been shown to produce similar effects [18]. Although the torsional pendulum technique used in that case did not allow the entire sorption/desorption process to be followed, the results presented there provide strong support for the notion that mechanosorptive phenomena are not limited to hygroscopic materials subjected to cyclically changing humidity conditions. Kubát and Lindbergson [18] give several examples of non-hygroscopic materials where the mechanical loss factor decreases during the sorption/desorption process, provided the surrounding atmosphere contains molecules capable of interacting with the specimen. For instance, this is the case with the systems polystyrene–benzene, rubber hydrochloride–chloroform and cellulose acetate–acetone.

The system poly(vinyl acetate)–acetone, where a distinct decrease of $\tan\delta$ was recorded with the pendulum device [18], deserves special mention. The absence of similar effects when studying the system PVAc–water in the present paper, demonstrates the importance of sufficient interaction between the specimen and the molecules constituting the environment.

These examples indicate that mechanosorptive effects in their conventional sense, that is primarily a distinct acceleration of the creep process when the atmosphere around the sample is varied, are to be expected for any system where there is sufficient interaction between the atmosphere and the specimen. A rough measure of this interaction is the solving or swelling power of the surrounding molecules. However, such generalizations of mechano-sorptive phenomena, including non-aqueous environments, do not appear to have been studied. A likely reason for this is the technically important preoccupation with wood and paper where water is a natural component.

A brief discussion of attempts to describe effects of this type can be found elsewhere [15]. The magnitude of the mechanical loss factor appears to be a measure of the internal mobility of the material. However, to increase the mobility, one does not have to rely on introducing or extracting foreign molecules into or from the material. Such an increase can be accomplished with the material as such, by simply applying a sufficiently high load. In fact, a transient increase in the damping capacity has been observed in the initial stages of creep and stress relaxation of high density polyethylene [19].

Needless to say, such an effect cannot be accommodated within the realm of linear viscoelasticity. This also applies to the results presented in this paper. Similar results of a more recent date have been reported for the primary creep of 17Cr ferritic stainless steel [20] and monocrystalline aluminium [21]. We conclude by mentioning a highly relevant result of a paper reporting on measurements of internal friction during tensile testing of glassy polycarbonate [22]: "It has been shown that internal friction is related to the density of mobile defects". This statement is certainly well in line with the findings of the present paper. For space reasons, sorption data relating to the materials used have not been included here. Their relation to the dynamic mechanical behaviour discussed here will be treated in a forthcoming publication.

Acknowledgements

The authors thank the Jacob Wallenberg Foundation for supporting this work, Professor Carl Klason for providing a favourable research environment, and Dr. D. H. McQueen, who took a highly active part in this work.

References

1. L. D. ARMSTRONG and R. S. T. KINGSTON, *Nature* **185** (1960) 860.
2. C. BOEHME and C. HARBS, *Holz Roh u. Werkstoff* **42** (1984) 335.
3. P. HOFFMEYER and R. W. DAVIDSON, *Wood Sci. Technol.* **23** (1989) 215.
4. A. RANTA-MAUNUS, *Mater. Struct.* **26** (1993) 362.
5. A. HANHIJÄRVI, Technical Research Centre of Finland, Espoo, paper 231 (VTT, 1995).
6. V. L. BYRD, *TAPPI J.* **53** (1972) 1612.
7. C. SÖREMARK and C. FELLERS, *J. Pulp Pap. Sci.* **19** (1993) J19.
8. H. W. HASLACH, *TAPPI J.* **77**(10) (1994) 179.
9. T. J. URBANIK and SUNG K. LEE, *Wood Fiber Sci.* **27** (1995) 1.
10. J. Z. WANG and D. A. DILLARD, *J. Compos. Mater.* **24** (1990) 994.
11. J. Z. WANG, D. A. DILLARD and T. C. WARD, *J. Polym. Sci. Part B* **30** (1992) 1391.
12. J. Z. WANG, D. A. DILLARD and F. A. KAMKE, *J. Mater. Sci.* **26** (1991) 5113.
13. Z. V. PADANYI, *Products Papermaking* **1** (1993) 521.
14. J. M. DINWOODIE, B. H. PAXTON, J. S. HIGGINS and D. J. ROBSON, *Wood Sci. Technol.* **26** (1991) 39.
15. R. P. EBRAHIMZADEH and D. G. KUBÁT, *J. Mater. Sci.* **28** (1993) 5668.
16. R. P. EBRAHIMZADEH, J. KUBÁT and D. H. McQUEEN, *Holz Roh u. Werkstoff* **54** (1996) 1.
17. V. DOUNIS, J. C. MORELAND, G. L. WILKES, D. A. DILLARD and R. B. TURNER, *J. Appl. Polym. Sci.* **50** (1993) 293.
18. J. KUBÁT and B. LINDBERGSON, *ibid.* **9** (1965) 2651.
19. J. KUBÁT, L. Å. NILSSON and M. RIGDAHL, *Rheol. Acta* **23** (1984) 40.
20. DONG-SHENG SUN, T. YAMANE, J. TAKAHASHI and K. MATSUSHITA, *J. Mater. Sci. Lett.* **12** (1993) 1172.
21. H. ZHOU and Q. P. KONG, *Scripta Mater.* **34** (1996) 269.
22. J. PARISOT, O. RAFI and W. J. CHORI, *Polym. Engng Sci.* **24** (1984) 886.

Received 28 May
and accepted 23 October 1996